



ANDRZEJ NOWAKOWSKI\*

**THE LAW OF EFFECTIVE STRESS FOR ROCKS IN LIGHT OF RESULTS OF LABORATORY EXPERIMENTS****PRAWO NAPRĘŻEŃ EFEKTYWNYCH DLA SKAŁ W ŚWIETLE WYNIKÓW BADAŃ LABORATORYJNYCH**

This paper presents the results of laboratory tests carried out in order to formulate effective stress law. The law was sought for two different cases: first – when rock was treated as a porous Biot medium (Biot, 1941; Nur & Byerlee, 1971) and second – when the law was formulated according to definition of Robin (1973) developed by Gustkiewicz (1990) and Nowakowski (2007). In the first case coefficients (4) and (5) of the Biot equation (3) were determined on the basis of compressibility test, in the second one effective pressure equation (9) and effective pressure value (11) were found on the basis of results of so called individual triaxial compression test (see Kovari et al., 1983) according to the methodology given by Nowakowski (2007).

On the basis of Biot coefficients set of values was found that volumetric strain of the pore space described by a coefficient (5) was not dependent on the type of pore fluid and the pore pressure of only, while in case of volumetric strain of total rock described by coefficient (4) both the structure and texture of rock were important.

The individual triaxial compression test results showed that for tested rock an effective pressure equation was a linear function of pore pressure as (15). The so called Rebinder effect (Rehbinder & Lichtman, 1957) might cause, that the  $\alpha$  coefficient in equation (15) could assume values greater than one. This happened particularly in the case when the porous fluid was non-inert carbon dioxide.

In case of inert pore fluid like kerosene the test results suggested that the  $\alpha$  coefficient in equation (15) decreased while the differential strength limit was increasing. This might be caused by, so called, dilatancy strengthening (see Zoback & Byerlee, 1975).

Another considered important parameter of the equation (15) was the value of the effective press  $p'$ . The results showed that the value of this parameter was practically independent on the pore fluid type. This conclusion was contrary to previous research (see, for example, Gustkiewicz et al., 2003 and Gustkiewicz, 1990) so these results should be treated with caution. There are no doubts, however, over  $p'$  increasing simultaneously with increase in  ${}^R\sigma_1 - \sigma_3$ . Basically, the differential strength limit of the specimen is greater the greater is confining pressure applied to it. Thus, higher  ${}^R\sigma_1 - \sigma_3$  values are accompanied by higher  $p'$ .

**Keywords:** effective stress law, conventional effective stress law, effective pressure equation, effective pressure value, Biot theory, Biot coefficient, compressibility test, triaxial compression test

\* STRATA MECHANICS RESEARCH INSTITUTE OF THE POLISH ACADEMY OF SCIENCES, UL. REYMONTA 27, 30-059 KRAKÓW, POLAND

W artykule przedstawiono wyniki badań laboratoryjnych wykonanych w celu sformułowania prawa naprężeń efektywnych, które prowadzono dla dwóch różnych sposobów formułowania tego prawa. W pierwszym przypadku zakładano, że skała jest ośrodkiem porowatym Biota (Biot, 1941; Nur i Byerlee, 1971), a samo prawo naprężeń efektywnych ma postać (3). W drugim przypadku posługiwano się podejściem zaproponowanym przez Robina (1973), które zostało następnie rozwinięte w Pracowni Odształceń Skał IMG PAN m.in. przez Gustkiewicza (1990) i Nowakowskiego (2007) i wyznaczano prawo naprężeń efektywnych składające się z dwóch elementów: równania ciśnienia efektywnego (9) oraz wartości ciśnienia efektywnego (11).

Podstawą wyznaczania współczynników dla równania Biota (3) były testy ściśliwości próbek skał pozostających w stanie powietrznie suchym oraz nasyconych inertywnymi (azot, nafta) bądź sorbującymi (dwutlenek węgla, woda destylowana) płynami porowymi. Na podstawie wyników tych testów wyznaczano moduły ściśliwości badanych skał a następnie wyliczano wartości współczynników Biota wg (4) i (5). Przedmiotem badań były próbki z naprężeń dwóch skał oznaczonych jako piaskowiec 8348 i wapień 9166.

Równanie ciśnienia efektywnego (9) oraz wartość ciśnienia efektywnego (11) wyznaczano wg metodyki podanej przez Nowakowskiego (2007) na podstawie wyników testu klasycznego trójosiowego ściskania (ang. „individual test” – por. Kovari i in., 1983) uzyskanych dla próbek skał, w których naprężenie różnicowe osiągnęło wartość różnicowej granicy wytrzymałości  ${}^R\sigma_1-\sigma_3$ . Przedmiotem badań były próbki wycięte ze skały oznaczonej jako piaskowiec „Tumlin”, a jako płynów porowych użyto azotu i nafty (płyny inertne) oraz dwutlenku węgla i wody destylowanej (płyny sorbujące).

Z przedstawionych wyników badań nad wartościami współczynników Biota wynika, że rodzaj płynu porowego nie wpływa na wartość wyznaczanego według wzoru (5) współczynnika  $a_2$  co oznacza, że deformacja objętościowa tej przestrzeni nie zależy od rodzaju płynu porowego, a jedynie od panującego w niej ciśnienia. W przypadku współczynnika  $a_1$  (wzór (4)) określającego wpływ ciśnienia porowego na deformację ośrodka jako całości wyniki wykazują pewną sprzeczność. Wartości  $a_1$  uzyskane dla piaskowca gdy płynem porowym jest nieściśliwa ciecz są nieco większe niż gdy jest nim ściśliwy gaz. Z kolei wyniki uzyskane dla opoki wskazują na coś wręcz przeciwnego: stosunkowo duża (większa niż dla piaskowca) wartość  $a_1$  dla gazu i wyraźnie mniejsze wartości  $a_1$  dla cieczy. Ostatecznie wydaje się, że to, czy wartość współczynnika  $a_1$  zależy rodzaju medium porowego jest w dużym stopniu uwarunkowane strukturą i teksturą badanej skały. Dla skał okruchowych o dużej porowatości i dużej swobodzie filtracji płynu porowego rodzaj tego płynu będzie miał prawdopodobnie mniejsze znaczenie natomiast dla skał zwartych o małej porowatości mogą zachodzić duże różnice w wartościach tego współczynnika w zależności od tego czy medium porowym jest ciecz, czy gaz.

Wyniki wykonanych testów konwencjonalnego trójosiowego ściskania pozwoliły stwierdzić, że dla badanego piaskowca równanie ciśnienia efektywnego na granicy wytrzymałości jest liniową funkcją ciśnienia porowego  $p_p$  postaci (15). Zgodnie z tym co pokazali Gustkiewicz i in. (2004) oraz Nowakowski (2005, 2007) jeżeli oddziaływanie płynu porowego na skałę nie jest wyłącznie mechaniczne, to może dojść do sytuacji, w której współczynnik  $\alpha$  w równaniu (15) ma wartość większą od 1. Zjawiskiem fizykochemicznym odpowiedzialnym za taką sytuację jest najprawdopodobniej tzw. efekt Rebinder'a (Rehbinder i Lichtman, 1957), który polega na obniżeniu wytrzymałości skały wskutek adsorpcji gazu porowego, przy czym spadek wytrzymałości jest tym większy, im wyższa jest ilość zasorbowanego gazu (por. także Hołda, 1990).

Jeżeli płynem porowym jest  $\text{CO}_2$  to im wyższa wartość  ${}^R\sigma_1-\sigma_3$  tym wyższa wartość  $\alpha$ , czyli tym silniej manifestuje się wpływ ciśnienia porowego (rys. 6). Przyczyną takiego zjawiska należy prawdopodobnie upatrywać w sposobie pękania badanego materiału. Jak wiadomo różnicowa granica wytrzymałości rośnie ze wzrostem ciśnienia okólnego oraz ze wzrostem różnicy  $p-p_p$  (Gustkiewicz, 1990). Wzrostowi temu towarzyszy stopniowa zmiana sposobu pękania skały od kruchego pękania do ciągliwego płynięcia. W próbce pękającej krucho wytwarza się zazwyczaj jedna płaszczyzna pęknięcia, wzdłuż której następuje zniszczenie próbki. Natomiast w próbce pękającej w sposób ciągliwy powstaje wiele równoległych do siebie płaszczyzn zniszczenia. Oznacza to, że sumaryczna powierzchnia nowych spękań powstających podczas zniszczenia ciągliwego jest prawdopodobnie znacznie większa niż podczas kruchego pęknięcia. Jeśli w trakcie eksperymentu spełnione są warunki (6) to pęknięcia te zostają wypełnione pozostającym pod stałym ciśnieniem gazem porowym, a to z kolei oznacza wzrost powierzchni fizykochemicznie czynnej, na której mogą zachodzić procesy sorpcyjne. A zatem i wpływ efektów sorpcyjnych powinien się okazać dla wyższych wartości  ${}^R\sigma_1-\sigma_3$  znacząco większy.

W przypadku, gdy płynem porowym była inercyjna ciecz (nafta) pokazane na rys. 6 wyniki badań sugerują, że wartość współczynnika  $\alpha$  maleje ze wzrostem  ${}^R\sigma_1-\sigma_3$ . Przyczyną może tu być tzw. wzmocnienie

dylatancyjne (por. Zoback i Byerlee, 1975). W tym przypadku polega ono na tym, że gdy próbka skalna osiąga swoją granicę wytrzymałości zaczynają się w niej rozwijać nowe spękania, czego konsekwencją jest wzrost objętości przestrzeni porowej wywołujący spadek ciśnienia porowego. Jeżeli spadek ten nie zostanie wyrównany przez filtrującą z zewnątrz ciecz to rzeczywista wartość ciśnienia porowego będzie niższa niż zakładana. Z punktu widzenia prawa ciśnienia efektywnego oznacza to, że wpływ ciśnienia porowego na wartość  ${}^R\sigma_1 - \sigma_3$ , ulegnie zmniejszeniu, co powinno dać  $\alpha < 1$ .

Drugim istotnym parametrem równania (15) jest tzw. wartość ciśnienia efektywnego  $p'$ . W rozważanych eksperymentach wielkość tę należy traktować jako pewne zastępcze ciśnienie okólne, które – zastosowane do skały dla  $p_p = 0$  – da w efekcie taką samą wartość  ${}^R\sigma_1 - \sigma_3$  jak para niezerowych ciśnień  $p$  i  $p_p$  spełniających równanie (15). Pokazane na rys. 7 zależności sugerują, że wartość wielkości  $p'$  praktycznie nie zależy od rodzaju płynu porowego. Innymi słowy: jeśli  $p_p = 0$  to  ${}^R\sigma_1 - \sigma_3 = const.$  dla danej wartości  $p'$  niezależnie od tego, czym wypełniona jest przestrzeń porowa skały. Wartości  $p'$  rosną natomiast ze wzrostem  ${}^R\sigma_1 - \sigma_3$  gdyż różnicowa granica wytrzymałości próbki jest tym wyższa im wyższe jest obciążające próbkę ciśnienie okólne. Jest zatem naturalne, że wyższym wartościom  ${}^R\sigma_1 - \sigma_3$  towarzyszą wyższe wartości  $p'$ .

**Słowa kluczowe:** prawo naprężeń efektywnych, konwencjonalne naprężenie efektywne, równanie ciśnienia efektywnego, wartość ciśnienia efektywnego, teoria Biota, współczynnik Biota, test ściśliwości, test trójosiowego ściskania

## Introduction

The notion of effective pressure emerged in continuum mechanics at the beginning of the XX century, once there was need to describe soil as porous medium whose pore space might be filled with pressurised pore fluid. This fluid might cause solely mechanical interactions involving change in rock mass stress due to changes in pore fluid pressure, as well as physiochemical and chemical transforming properties of rock mass through interaction between the fluid and groundmass (e.g. sorption, chemical reactions). In more complicated instances, those factors could even combine with each other.

Once the aforementioned problem surfaced it became clear that mathematical description of processes taking place in loaded porous medium, whose pore space is filled with pressurised fluid would require to first derive mathematical formulae for pore space itself. Bearing in mind they would have to include information about the size and shape of pores, their distribution across analysed space and whether they create a network of connections or are just isolated cavities, it should come as no surprise that deriving such mathematical description has been deemed impossible. Hence it was suggested to assume soil to be a homogeneous and isotropic porous medium, filled completely with pressurised pore fluid (pore pressure  $p_p$ ) and remaining under macroscopic stress  $\sigma_{ij}$ . Then, it was further suggested to formulate relationships describing stress and strain within the medium for substitute stress  $'\sigma_{ij}$  called **effective stress**. It was further assumed the effective stress is a function of macroscopic stress and pore fluid pressure i.e.:

$$'\sigma_{ij} = f(\sigma_{ij}, p_p) \quad (1)$$

Note that in Anglo-Saxon literature the above-mentioned relationship is often referred to as the **law of effective stress** (see e.g. Patterson and Wong, 2005; p. 148 and further), and for purposes of this paper that term will prevail.

# 1. Mathematical description of the law of effective stress

Numerous interesting facts about the history of searching for the ultimate form of the formula (1) could be found e.g. in work by Bluhm and de Boer (1996) as well as Lade and de Boer (1997). The concepts used in these papers have been described in brief below.

## 1.1. Conventional effective stress

First legitimate research into impact of pore fluid pressure on mechanical properties of porous medium was conducted by Paul Fillunger (Fillunger, 1915, 1914, 1913) at Vienna University of Technology at the beginning of the XX century. Unfortunately character traits of the scholar and his long-lasting clash with Karl von Terzaghi tied in with international popularity of the latter (see de Boer, 2005) meant Paul Fillunger went on to be virtually forgotten, whilst Karl von Terzaghi became widely acknowledged as the driving force behind the concept of effective stresses.

It is dated back to 1923 (Terzaghi, 1923), however, the law of effective stresses itself became his brainchild *explicité* as late as in 1936 (Terzaghi, 1936). It states that if:  $\sigma_{ij}$  – macroscopic stress tensor,  $'\sigma_{ij}$  – effective stress tensor,  $p_p$  – pore pressure and  $\delta_{ij}$  – Kronecker symbol the equation (1) becomes:

$$'\sigma_{ij} = \sigma_{ij} - p_p \delta_{ij} \quad (2)$$

At the current time, the law of effective stress in that form is referred to as the **conventional effective stress law** (see Paterson & Wong, 2005, p. 148).

The equation (2) was derived for the very first time by von Terzaghi while he was working over consolidation of clayey soil layers and seemingly it was a product of intuitive calculations (see de Boer & Ehlers, 1990), hence the author did not determine its range of applications. Further down the line it was proven, there are specific limits.

Limits of application produced by the formula (2) were determined over the course of experiments carried out in 1963 by research team led by John Handin. That team, drawing on laboratory tests of five rocks: dolomite, limestone, sandstone, shale and fine-grained sandstone came up with three conditions which are ought to be satisfied should the law of effective stress (2) be applied to a porous medium. They are as follows (citation Handin et al., 1963):

- (a) the interstitial fluid is inert relative to the mineral constituents of the rock so that pore pressure effects are purely mechanical,
- (b) the permeability is sufficient to allow pervasion of the fluid and furthermore to permit the interstitial fluid to flow freely in or out of the rock during the deformation so that the pore pressure remains constant and uniform throughout (the test is “drained”),
- (c) the rock is a sandlike aggregate with connected pore spaces, the configuration of which insures that the pore (“neutral”) pressure is transmitted fully throughout the solid phase.

The conditions cited above (a), (b) and (c) will be hereunder referred to as – for interest of simplicity – “Handin conditions”.

As far as theoretical considerations are concerned, the final word belongs to the most conclusive paper by Bluhm and de Boer (1996), in which the authors – through analysing theory of mixtures equations – arrived at conclusion the conventional effective stress law holds solely for specific case of incompressible porous medium whose pore space is filled only by incompressible and inviscid pore fluid.

## 1.2. The effective stress as linear function of pore pressure and stress

By searching for a more universal effective stress law, the equation (2) was proposed to be changed into:

$$\sigma'_{ij} = \sigma_{ij} - \alpha p_p \delta_{ij} \quad (3)$$

where  $\alpha$  is a dimensionless coefficient determining how much of pore pressure should be taken into account for the equation (3) to become a relationship describing effective pressure.

The effective stress law in form (3) automatically triggers question as to the value of the  $\alpha$  coefficient. For purposes of this paper the proposition put forward in 1940 by Maurice Biot is the most significant. It was published in his consolidation theory (Biot, 1941). Central for that solution was introducing to Hooke's law equations elements factoring in elastic and volumetric soil deformation and adding another equation taking into account pore pressure.

Nur and Byerlee (1971) showed through developing the Biot's concept that if the analysed medium is under hydrostatic pressure within limits of its elastic deformation, the  $\alpha$  coefficient could be derived using experimentally determined medium's porosity ( $n$ ), bulk modulus ( $K$ ) and bulk modulus of its solid phase ( $K_S$ ). The  $\alpha$  coefficient is expressed by the following relationships:

$$\alpha_1 = 1 - \frac{K}{K_S} \quad (4)$$

when effective pressure equation is formulated for changing volume of analysed medium as a whole (i.e. solid phase + pore space), and on the other hand

$$\alpha_2 = 1 - \frac{nK}{K_S - K} \quad (5)$$

when effective pressure equation is formulated solely for pore space of the medium.

Nur and Byerlee's take on the Biot's concept, although mathematically very neat indeed, introduced substantial limitations to the study of effective pressure. One should bear in mind that Biot's equations are in essence expanded Hooke's law equations (see Paterson & Wong, 2005 – pp. 149-152; Fabre & Gustkiewicz, 1998), hence their applicability as constituent equation for porous medium overlaps with that of Hooke's law. This is an important caveat, because Hooke's set of equations could only be used as constituent equations for a limited range of stresses.

## 1.3. The law of effective stress based on conventional triaxial compression test

The last method of approaching effective stresses used for purposes of this paper was developed at The Laboratory of Rock Deformation of The Strata Mechanics Research Institute in Kraków, which uses findings provided by laboratory experiments into rocks under conventional triaxial state of stress (the so-called "individual test" – see Kovári et al., 1983). The inspiration behind that method were theories formulated by Robin (1973). Nowakowski (2007) in turn described

in great detail research methodology and how to use its results to determine the law of effective stresses. In this paper only the fundamentals of proposed approach are to be presented.

Square one of this method are results of triaxial compression test carried out using a rock cylinder specimen, whose pore space was filled with pressurised pore fluid (either gas or liquid). During the test the specimen is placed in Kármán type triaxial cell and is loaded with axially-symmetrical compressive stress<sup>1</sup> satisfying  $\sigma_1 \geq \sigma_2 = \sigma_3 = p$ . The confining pressure  $\sigma_2 = \sigma_3 = p$  is applied to specimen's side surface by liquid, and axial stress ( $\sigma_1$ ) by hydraulic piston pressing against the specimen's face. The pore fluid remains under constant pressure  $p_p$ . Both the chamber and the pore space are connected to external sources of pressure in order to satisfy the conditions:

$$p = \text{const} \quad \wedge \quad p_p = \text{const} \quad (6)$$

Experiment conditions require pressures  $p$  and  $p_p$  to satisfy the following condition (see Gustkiewicz et al., 2004, 2003):

$$p - p_p \geq 0 \quad (7)$$

thus the pore pressure can equal the confining pressure at the most.

Following that procedure, the test can return any  $Q$  quantity, which is the function of pressures  $p$  and  $p_p$ . Within the space of variables ( $Q, p, p_p$ ) that function creates a surface where a curve satisfying the equation is found:

$$Q(p, p_p) = \text{const} \quad (8)$$

This equation produces the curve across which the interesting to us  $Q$  quantity is constant. By projecting the curve (8) on plane ( $p_p, p$ ), a relationship is produced on that plane given by equation:

$$f(p, p_p) = 0 \quad (9)$$

By substituting to equation (9):

$$p_p = 0 \quad (10)$$

we get

$$f(p, 0) = p' = \text{const} \quad (11)$$

The equation (9) defining set of points  $p$  paired with  $p_p$  for which the  $Q$  quantity is constant, will hereunder be referred to as **effective pressure equation**, and defined by formula (11) pressure  $p'$  **effective pressure value** for effective pressure equation (9) and quantity  $Q$  satisfying the condition (8). For the ultimately produced  $p'$  pressure the following is satisfied:

$$Q(p', 0) = Q(p') = Q' = \text{const} \quad (12)$$

<sup>1</sup> In this paper the notations are: „plus“ for compression and „minus“ for tension.

Note at this point that the above-obtained effective pressure law does not consist of a single equation – its constituent components are equation (9) and constant (11). The equation (9) defines the relationship between the confining pressure and pore pressure necessary to satisfy the condition (8), whereas the constant (11) provides a substitute confining pressure, which – for rock at  $p_p = 0$  – has the same influence on the  $Q$  quantity as the pair of non-zero pressures  $p$  and  $p_p$  satisfying the relationship (8) and (9) does.

The presented formalism of describing the effective pressure was proposed for the first time by Robin (1973). Gustkiewicz (1990) provided methodology to analyse phenomena occurring in rock specimens where the stress reached the differential strength limit. It was further developed by Gustkiewicz himself (Gustkiewicz, 1990) and others (Gustkiewicz et al., 2003, 2004) and Nowakowski (2005). The research methodology has been described in detail by Nowakowski (2007). Based on work carried out by those authors, it is fair to conclude the effective pressure equation (11) will depend among others on:

- analysed  $Q$  quantity,
- state of stress in the rock,
- properties of rock's pore space.

The aforementioned Robin (1973) did make the comment that in practice finding correct form of equation (11) entails usually going through convoluted and tedious laboratory experiments whose findings might prove inconclusive.

## 2. Solving for Biot's coefficients based on experimental study

When discussed was – in chapter 1.2 of this paper – the law of effective stress according to Biot – Nur and Byerlee, the procedure used by those authors to obtain relationships (4) and (5) was neglected. Close inspection of that procedure (e.g. how Dutka and others did, 2008) shows, that the effective stress is the stress controlling changes in medium's volume (and/or its pore space) depending on macroscopic stress and pore pressure. This is clear from relationships (4) and (5). The material constants  $K$  and  $K_S$  they include are quantities linking together medium stresses with volume changes.

### 2.1. Methodology of carried out laboratory experiments

In order to compute Biot's coefficients necessary for the equation (3) the following material constants had to be determined:

- porosity ( $n$ ),
- bulk modulus of rock ( $K$ ),
- bulk modulus of rock solid phase ( $K_S$ ).

Rock porosity – pore space per total volume of the rock – determined using intermediate method, where bulk density of rock  $\rho$  and specific density of rock  $\rho_S$ , and the following was used:

$$n = 1 - \frac{\rho}{\rho_S} \quad (13)$$

Required densities were measured using pycnometers:  $\rho$  – GeoPyc 1360 Envelope Density Analyzer,  $\rho_S$  – AccuPyc II 1340 Gas Displacement Pycnometry System. Both devices are currently owned by the Laboratory of Micrometrics of IMG PAN.

Bulk moduli were determined directly by conducting the so-called compressibility test, which involves compressing rock specimen by applying hydrostatic pressure ( $p$ ) whilst measuring volumetric strain ( $e$ ). The bulk modulus is given by tangent of angle between rectilinear part of plot  $p(e)$  and strain axis.

The  $K$  modulus is determined through the compressibility experiment, where the pore space is open and pore pressure equals barometric pressure (by convention this is given by  $p_p = 0$ , although that is inaccurate). Then the strain in analysed specimen is the sum of strain in its matrix and pores. It is easy to conclude that the higher the porosity of rock the higher the strain thus the lower the  $K$  modulus.

The compressibility test is used to determine the  $K_S$  modulus, where the pore pressure constantly equals the hydrostatic pressure ( $p_p = p$ ). Note that the entire pore space should be filled with pore fluid. This means the computational error when determining the  $K_S$  increases with percentage of the so-called isolated pores i.e. pores without connections with other cavities surrounded completely by rock mass. Detailed information concerning procedures of carrying out the aforementioned compressibility experiments at the Laboratory of Rock Deformation of IMG PAN are given in Gustkiewicz's paper (1989).

At this stage it must be emphasized that neither Biot nor Nur, Byerlee or indeed any other – to the author's best knowledge – paper concerning this subject matter (e.g.: Rice & Cleary, 1976; Zienkiewicz & Shiomi, 1984; Detournay & Cheng, 1993; Roegiers and others, 1998; Lade & de Boer, 1997) is conclusive as to the packing material for pore space during the compressibility test. The referred to on numerous occasions Gustkiewicz (1989) suggests to determine the  $K$  modulus when the pore space is filled with air (dry air state). The  $K_S$  on the other hand when it is filled with kerosene. Even this author, however, takes no interest in considering the impact of the fluid type on test results. Hence, a decision was made to mark  $K$  and  $K_S$  moduli on rock specimens whose pore space was filled with different pore fluids – both liquids and gases. Experimentally determined bulk moduli were then used to determine Biot's coefficients  $\alpha_1$  and  $\alpha_2$  given by equations (4) and (5).

## 2.2. Results of laboratory experiments

Selected for research were two rocks provided by Institute of Geonics of the Academy of Sciences of the Czech Republic: sandstone – henceforth referred to as “sandstone 8348”, and gaize – “gaize 9166”. The sandstone was a sedimentary rock of ashen-yellow colour, bonded with cement, medium-grained, poorly sorted. The limestone was created chemically (precipitation) by combining carbonate phase and silica (opal, chalcidon) into a compact matrix (carbonate components did not leach).

Common practice in determining Biot's coefficients is to assume the following, mean porosities (acquired through pycnometer measurements):

- for sandstone 8348                      –  $n_p = 15.9\%$  (standard deviation 0.81%),
- for limestone 9166                     –  $n_o = 7.4\%$  (standard deviation 1.22%).

Both series contained 16 specimens.

In order to assess influence of pore fluid on Biot's coefficients a series of compressibility tests were carried out. Pore fluids were:

- b) kerosene – inert liquid,
- c) distilled water (H<sub>2</sub>O) – non-inert liquid,
- d) nitrogen (N<sub>2</sub>) – inert gas,
- e) carbon dioxide (CO<sub>2</sub>) – non-inert gas,

The compressibility test was carried out for the above-mentioned pore fluids under the following conditions: pore pressure equal to barometric pressure ( $p_p = 0$ ); pore pressure equal to hydrostatic pressure ( $p_p = p$ ). Determined through those experiments bulk moduli ( $K$  and  $K_S$  respectively) were then used to determine Biot's coefficients according to formulae (4) and (5). Figure 1 below shows an example result of compressibility test and consequently obtained Biot's coefficients, and then – tab. 1 and 2 – collates experimentally obtained  $K$ ,  $K_S$ ,  $\alpha_1$  and  $\alpha_2$  quantities.

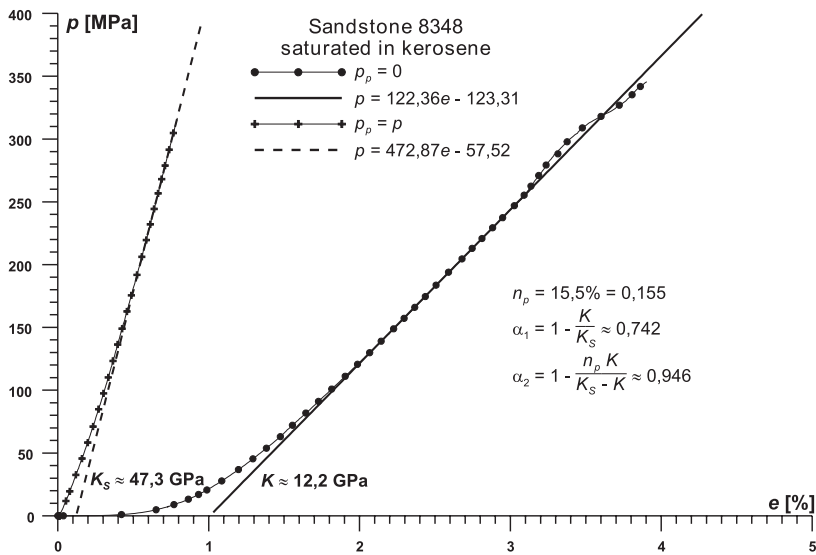


Fig. 1. Compressibility test results: kerosene saturated sandstone 8348

Analysis of quantities  $\alpha_1$  and  $\alpha_2$  presented in tab. 1 and 2 concludes that neither the type of rock nor pore fluid have any significant influence on the  $\alpha_2$  quantity (derived using the formula (5)) averaging  $0.925 \pm 0.034$ . Hence the effective pressure law derived for pore space will become as follows:

$$\sigma'_{ij} = \sigma_{ij} - 0,925 p_p \delta_{ij} \tag{14}$$

and its form is independent of the pore fluid type.

TABLE 1

Bulk moduli and Biot coefficients; sandstone 8348

		Sandstone 8348						
		$n_p$ [%]	$K$ [MPa]	$K_S$ [MPa]	$K : K_S$	$\alpha_1$	$\alpha_2$	$\alpha_1 : \alpha_2$
pore fluid	kerosene	15,5	12,2	47,3	1 : 3,9	0,742	0,946	1 : 1,3
	H <sub>2</sub> O		12,0	41,9	1 : 3,5	0,714	0,938	1 : 1,3
	N <sub>2</sub>		9,5	25,6	1 : 2,7	0,629	0,909	1 : 1,5
	CO <sub>2</sub>		13,2	38,1	1 : 2,9	0,653	0,917	1 : 1,4

TABLE 2

Bulk moduli and Biot coefficients; limestone 9166

		Limestone 9166						
		$n_o$ [%]	$K$ [MPa]	$K_S$ [MPa]	$K : K_S$	$\alpha_1$	$\alpha_2$	$\alpha_1 : \alpha_2$
pore fluid	kerosene	7,6	14,4	28,8	1 : 2,0	0,493	0,923	1 : 1,9
	H <sub>2</sub> O		21,5	33,6	1 : 1,6	0,360	0,865	1 : 2,4
	N <sub>2</sub>		12,8	54,0	1 : 2,4	0,763	0,976	1 : 1,3
	CO <sub>2</sub>							

In case of the  $\alpha_1$  coefficient the situation was more complicated and depended on the type of rock. Hence, values of the  $\alpha_1$  quantity were slightly greater for liquid pore fluid. The contrary was true for the limestone: the  $\alpha_1$  coefficient was greater for gas pore fluid. Possible reasons behind such state of affairs are discussed in chapter 4.1.

### 3. Determining the effective pressure law based on conventional triaxial compression tests

This chapter discusses results of research into effective pressure law concentrating on analysing the  $Q$  rock's property (see chapter 1.3) of differential strength limit  $^R\sigma_1 - \sigma_3$  (for formal definitions see e.g. Gustkiewicz, 1990). Effective pressure equations (9) and corresponding pressure values (11) were searched for inert (kerosene, nitrogen) and non-inert (distilled water, carbon dioxide) pore fluids.

#### 3.1. Laboratory equipment and testing method

The conventional triaxial compression test was carried out using owned by the Laboratory of Rock Deformation of IMG PAN GTA-10 machine. It enables triaxial compression tests for confining pressure  $p \leq 400$  MPa and pore pressure  $p_p \leq p$ . The maximum loading force of the hydraulic press is 150 kN. Fig. 2 shows schematically the specimen under triaxial compression. Fig. 3 shows the machine itself.

The following quantities were registered during the test: applied loading force, piston displacement, specimen circumference change, confining pressure and pore pressure. Based on registered quantities computed were: longitudinal strain  $\varepsilon_1$ , transverse strain  $\varepsilon_3$  and volumetric

strain  $e$  of a specimen and differential stress  $\sigma_1 - \sigma_3$ . Also produced were charts of relationships between differential stress and corresponding strains. Those plots were then used to compute the above-mentioned differential strength limit of rock  ${}^R\sigma_1 - \sigma_3$ . It should also be pointed out that each  ${}^R\sigma_1 - \sigma_3$  value corresponds to one and one only pair of  $p$  and  $p_p$  pressures.

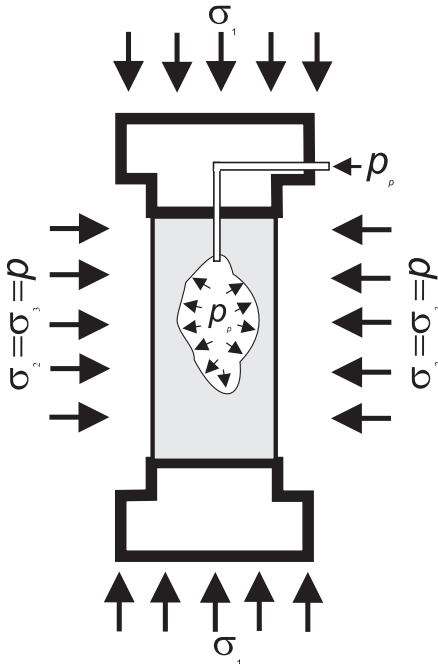


Fig. 2. Conventional triaxial compression test – the load case (Nowakowski, 2007)

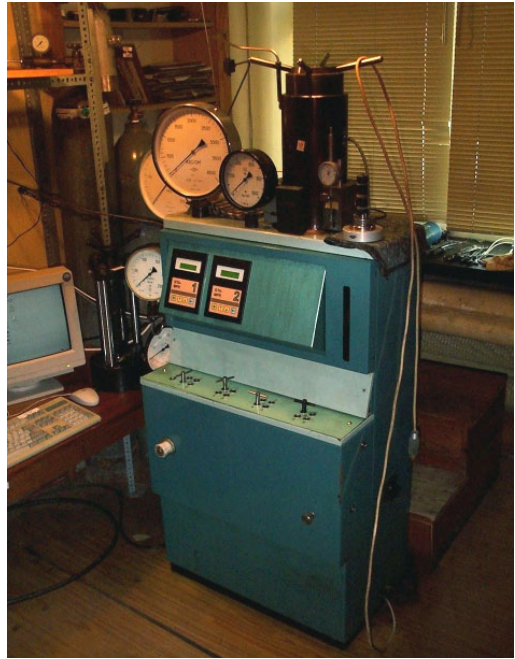


Fig. 3. The GTA-10 machine – general view (Gustkiewicz & Nowakowski, 2004)

Subsequently the experimentally obtained  ${}^R\sigma_1 - \sigma_3$  values were used plot the relationship between differential strength limit and pore pressure at given confining pressure. On the plane ( ${}^R\sigma_1 - \sigma_3, p_p$ ) this plot was a set of bell-shaped curves, where each of the curve corresponded to different confining pressure  $p$ . The next step was to select  ${}^R\sigma_1 - \sigma_3$  values for deriving equations (9) and computing values (11). Then straights  ${}^R\sigma_1 - \sigma_3 = \text{const}$  were added to the plot ( ${}^R\sigma_1 - \sigma_3, p_p$ ). Abscissas of intersecting straights with bell-shaped curves satisfying  $p = \text{const}$  returned for each  ${}^R\sigma_1 - \sigma_3$  a set of point pairs ( $p_p, p$ ) enabling to solve for equation (9) and values (11). The methodology outlined above has been described in detailed in paper by Nowakowski (2007).

### 3.2. The law of effective stresses for differential strength limit – the “Tumlin” sandstone

The Lower Triassic sandstone from Tumlin can be found in Northern part of Swietokrzyskie Mountains near Suchedniow. It is a medium-grained rock composed mainly of quartz grains and

clay minerals. 80% of the quartz are 40-1200  $\mu\text{m}$  isometric grains. The binder is predominantly quartz with admixtures of claystone. Detailed petrographic description of the sandstone can be found in paper by Nowakowski et al., (2003).

For purposes of the triaxial compression tests, the specimens were prepared as cylinders of  $d = 22$  mm diameter and  $h = 44$  mm height. Confining pressure used for the experiment was  $p = \{20 \text{ MPa}, 40 \text{ MPa}, 60 \text{ MPa}, 80 \text{ MPa}, 100 \text{ MPa}\}$ . Pore pressures were the same. Pore fluids were inert fluids (kerosene and nitrogen) and non-inert (distilled water and carbon dioxide). Equations and effective pressure values were computed for  $R\sigma_{1-\sigma_3} = \{100 \text{ MPa}, 150 \text{ MPa}, 200 \text{ MPa}, 250 \text{ MPa}, 300 \text{ MPa}\}$

Fig. 4 shows the relationship between differential strength limit ( $R\sigma_{1-\sigma_3}$ ) and specimen pore pressure ( $p_p$ ) at confining pressure ( $p$ ) i.e. the parameter obtained for kerosene impregnated "Tumlin" sandstone specimens. Shown in the figure bell-shaped curves were obtained through approximating experiment results with second-degree polynomial selected to make tangent to the bell-shaped curve a straight line horizontal at intersection with ordinates axis. Also plotted (solid line) were horizontal straight lines described by  $R\sigma_{1-\sigma_3} = \text{const}$  for specific values of differential strength limit for which effective pressure values and equation were determined.

Fig. 5 shows on plane ( $p_p, p$ ) sets of points were  $R\sigma_{1-\sigma_3} = \text{const}$  straight lines intersect with  $p = \text{const}$  bell-shaped curves required to derive – through approximation – effective pressure

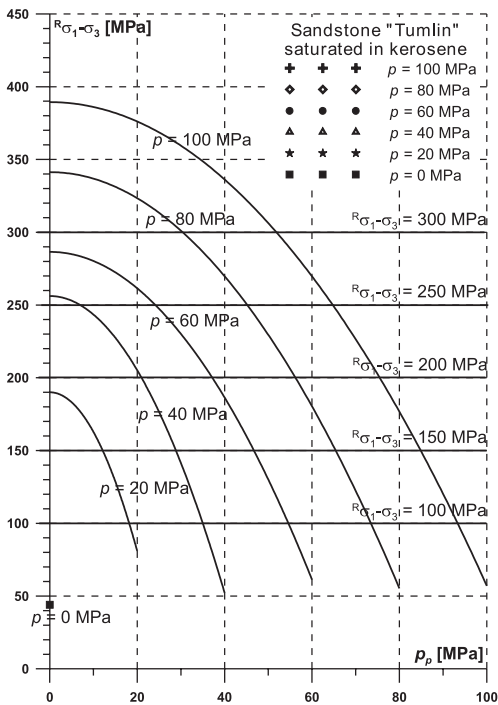


Fig. 4. Differential strength limit as function of pore pressure with confining pressure as parameter; kerosene-saturated "Tumlin" sandstone

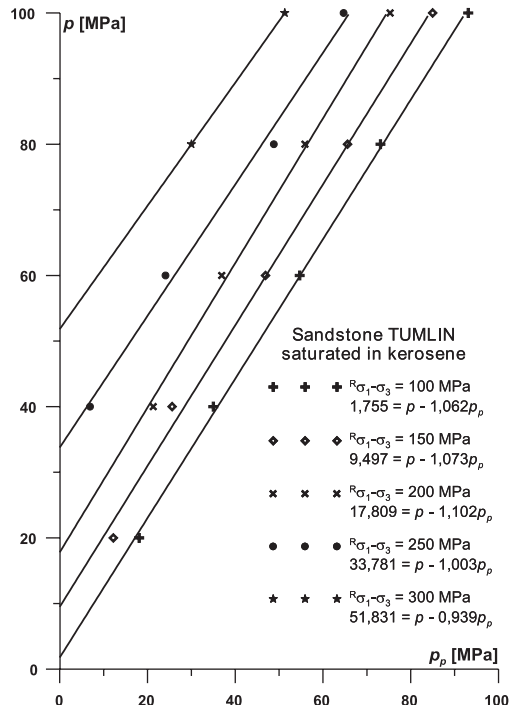


Fig. 5. Effective pressure equation and effective pressure value for different differential strength limits; kerosene-impregnated "Tumlin" sandstone

equations (9). The legend gives  ${}^R\sigma_1-\sigma_3$  values and corresponding effective pressure equation. Note that for all analysed  ${}^R\sigma_1-\sigma_3$  values the equation was:

$$p' = p - \alpha p_p \quad (15)$$

i.e. it was a linear function of confining pressure and pore pressure. The effective pressure value  $p'$  on the left-hand side of equation is in fact an coordinate of point where the straight (15) intersects with axis  $p$ .

The exact same procedure was then repeated to analyse results for the nitrogen-impregnated "Tumlin" sandstone and the remaining pore fluids i.e. distilled water and carbon dioxide. Each time the effective pressure equation was (15). Below – tab. 3 – presented are the  $\alpha$  coefficient values in effective pressure equations (15) and effective pressure values  $p'$  returned by those equations for individual  ${}^R\sigma_1-\sigma_3$  values and different pore fluids. Those quantities have been charted:  $\alpha$  coefficient – fig. 6 and effective pressure values  $p'$  – fig. 7.

Obtained results prove that gas pore fluid causes the  $\alpha$  coefficient to increase regularly in tandem with the differential strength limit (fig. 6). That rise is relatively insignificant for nitrogen and substantial for carbon dioxide. In case of both gases  $\alpha$  values are greater than unity.

Provided the pore medium jest liquid, observed relationships show little regularity, the caveat being that if for distilled water an upward trend of the  $\alpha$  is clear, this could not be said for kerosene –  $\alpha$  seems to be decreasing as the differential strength limit grows.

In case of effective pressure value  $p'$  (fig. 7) the case is clear and growing value of  ${}^R\sigma_1-\sigma_3$  translates into regular  $p'$  growth. That tendency is independent of the pore fluid type.

TABLE 3

The  $\alpha$  coefficient and effective pressure value  $p'$  for different pore fluids and different values of  ${}^R\sigma_1-\sigma_3$

		Pore fluid			
		kerosene	nitrogen	distilled water	carbon dioxide
${}^R\sigma_1-\sigma_3 = 100$ MPa	$\alpha$	1,062	0,968	1,054	1,064
	$p'$ [MPa]	1,8	5,8	3,4	2,6
${}^R\sigma_1-\sigma_3 = 150$ MPa	$\alpha$	1,073	1,024	0,979	1,133
	$p'$ [MPa]	9,5	10,0	12,9	7,6
${}^R\sigma_1-\sigma_3 = 200$ MPa	$\alpha$	1,102	1,055	1,095	1,201
	$p'$ [MPa]	17,8	17,5	18,7	15,6
${}^R\sigma_1-\sigma_3 = 250$ MPa	$\alpha$	1,003	1,073	1,096	1,254
	$p'$ [MPa]	33,8	29,5	30,3	28,8
${}^R\sigma_1-\sigma_3 = 300$ MPa	$\alpha$	0,939	1,117	1,282	1,307
	$p'$ [MPa]	51,8	42,7	35,9	50,6

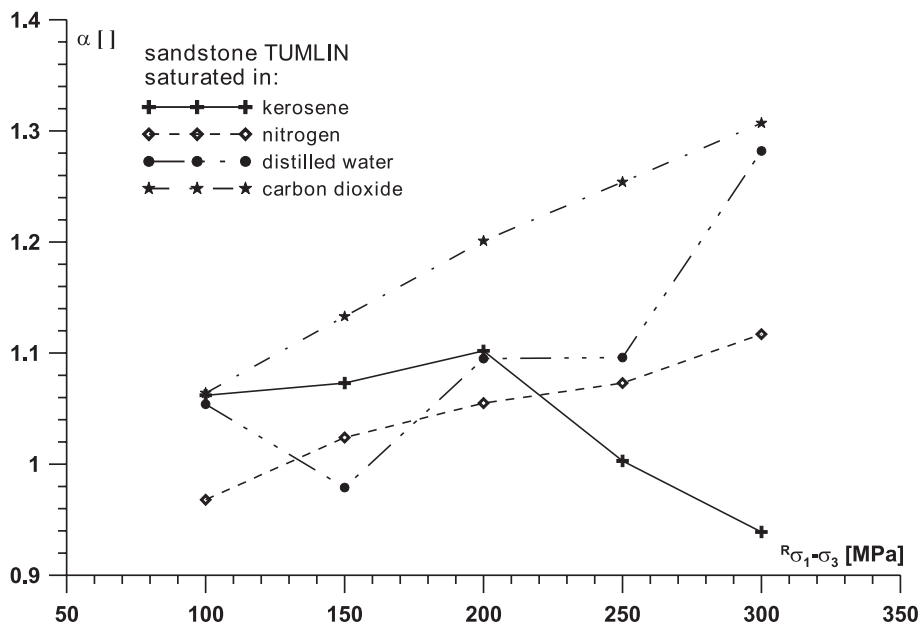


Fig. 6. Value of the  $\alpha$  coefficient for different values of  $R_{\sigma_1-\sigma_3}$  and different pore fluids; “Tumlin” sandstone

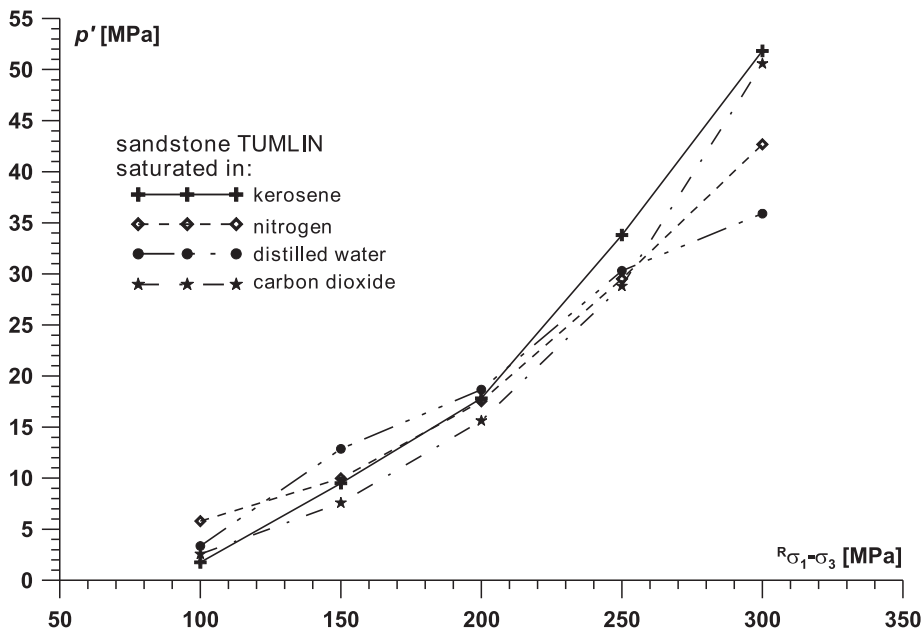


Fig. 7. Effective pressure value  $p'$  for different values of  $R_{\sigma_1-\sigma_3}$  and different pore fluids; “Tumlin” sandstone

## 4. Experimental study. Discussion

### 4.1. The relationship between Biot's coefficients and the type of pore fluid

The discussion concerning results of research into Biot's coefficients should get off to a good start by concluding (see final passages of chapter 2.2) the type of pore fluid does not influence the Biot's coefficient  $\alpha_2$  derived using the formula (5). Bearing in mind this coefficient should describe how does pore pressure impact on volumetric strain of pore space it seems fair to assume volumetric strain of pore space does not depend on the type of pore fluid, but on the pore pressure.

This fails to hold in case of the coefficient  $\alpha_1$  (formula (4)) which determines the impact of pore pressure on volumetric deformation of the entire medium. These results are even contradictory to an extent. Values of  $\alpha_1$  obtained for sandstone are slightly greater provided the pore fluid is an incompressible liquid than for compressible gas, however, the discrepancies – by our own admission – are not significant. On the other hand, results for the limestone indicate the opposite: relatively high (greater than for the sandstone)  $\alpha_1$  value for gas and considerably smaller  $\alpha_1$  for the liquid.

In accordance with (4) the  $\alpha_1$  coefficient should decrease as the  $K$  modulus increases and increase as the  $K_S$  modulus increases. We cannot rule out that during the compressibility test inside the sandstone specimen – pore space filled with liquid – closed cracks caused slippage (lubricating effect). This could consequently lead to higher strains and lower  $K$  module values. Ultimately the obtained  $\alpha_1$  values were “too high” in relation to gas acting as pore fluid.

Furthermore the key factors determining values of  $K$  and  $K_S$  moduli (and consequently of  $\alpha_1$  as well) are: fill-up fraction of pore space with pore fluid and feasibility of filtering the fluid in the cavity. Consequently the conditions required to determine the  $K_S$  modulus are: pores completely filled with fluid and its “speedy” filtration – required to maintain equal confining and pore pressures (see key paper by Gustkiewicz, 1989).

Measurements of kinetics whilst filling the pore space with gas and sorptive measurements (Dutka et al., 2008) carried out as part of preparations for compressibility tests proved that in case of sandstone specimen complete fill of pore space with inert gas (He) took just over 3 min. In case of absorbing gas (CO<sub>2</sub>) that time was longer i.e. approx. 50 min. until the state of sorption balance was reached (which took place far later than complete fill of pore space).

In case of limestone helium was not used as the packing material, but filling 50% of pore space with CO<sub>2</sub> took approx. 120 min. Interestingly, there were no sorptive effects taking place which could impact that process. Hence, firstly – in case of limestone there is no guarantee the entire specimen's pore space was filled with pore gas, secondly – even if the entire pore space was filled with gas, the filtration processes are sluggish enough to make maintaining  $p = p_p$  during the compressibility test impossible. Thereby the  $K_S$  modulus could not be determined correctly. Note that if filling the limestone with gas was that difficult, filling it with liquid must have been more troublesome, *ergo* empirical  $K_S$  values must have been weighed down with greater error than in case of gas used as pore fluid.

To summarise the above deliberations it is fair to say that dependence of Biot's coefficient  $\alpha_1$  on pore medium is to a significant extent contingent on the structure and texture of analysed rock. In case of rock of high porosity where pore fluid filters easily, type of that fluid plays a lesser role, whereas in case of rock of low porosity coefficient values might diverge significantly depending whether gas or liquid was used as the pore medium.

## 4.2. Impact of pore fluid type and phenomena taking place at the strength limit of rock on the effective pressure law

Results of carried out conventional triaxial compression tests concluded that for analysed sandstone the effective pressure law upon strength limit is a linear function of pore pressure  $p_p$  (15). There are two key parameters in that equation: effective pressure value  $p'$  and slope of straight line  $\alpha$ , but the  $\alpha$  coefficient in this equation operates as "weight" determining impact of pore pressure on the ultimate effective pressure value. First Gustkiewicz et al. (2004) and then Nowakowski (2005, 2007) proved that if pore fluid causes other interactions than solely mechanical, then  $\alpha$  might become greater than 1. A physiochemical phenomenon responsible for this is most probably the so-called Rehbinder effect (Rehbinder and Lichtman, 1957), where surface tension decreases as does the rock's strength due to absorption of pore gas. The greater the amount of absorbed gas the greater the decrease in strength (see Holda, 1990). Presented in fig. 6 relationships between differential strength limit  $^R\sigma_1-\sigma_3$  and corresponding  $\alpha$  values seem to suggest that if the pore fluid is an absorbing gas (carbon dioxide) then the above-mentioned situation occurs.

By analysing fig. 6 another observation can be made that if pore fluid is  $\text{CO}_2$  then the greater the  $^R\sigma_1-\sigma_3$  the greater the  $\alpha$  i.e. the impact of pore pressure is clearer. Reasons behind that phenomenon could be found in cracking pattern of tested material. According to common knowledge the differential strength limit increases as the confining pressure increases as well as the  $p - p_p$  difference (Gustkiewicz, 1990). That increase is accompanied by gradual change in cracking pattern from brittle failure to ductile flow. A brittle specimen usually cracks across a single plane i.e. where the specimen failure occurs. The specimen cracking in a ductile way on the other hand exhibits numerous parallel failure planes. This means that the total plane of new cracks occurring upon ductile failure is most probably much wider than during brittle cracking. Provided the conditions (6) are satisfied during the experiment, those cracks are filled with constant pressure pore gas and this in turn means greater non-inert surface, where sorptive processes can take place. Hence the impact of sorptive effects should prove considerable greater for higher  $^R\sigma_1-\sigma_3$  values.

Note that presented in fig. 6 relationship between  $\alpha$  and  $^R\sigma_1-\sigma_3$  obtained for nitrogen is equivalent to the same relationship for carbon dioxide even though nitrogen for sandstone should be an inert gas. It is not out of the question, that assuming nitrogen to be inert was an error, since the gas found in regular gas cylinders contains some water vapour, which is not inert. This would explain the qualitative similarity of given relationships for nitrogen and carbon dioxide, bearing in mind quantitatively the reaction of tested sandstone to nitrogen is considerably weaker.

In case where pore fluid was an inert liquid (kerosene), research results shown in fig. 6 suggest  $\alpha$  decreases as  $^R\sigma_1-\sigma_3$  increases. The so-called dilatant strengthening could be the reason here (see Zoback & Byerlee, 1975). In this case it involves the rock specimen reaching its strength limit thus causing new cracks to appear. Consequently the volume of pore space increases causing pore pressure to drop. Should it fail to be compensated through filtration with external liquid (the conditions (6) could not be satisfied), the actual pore pressure will be lower than assumed. According to the effective pressure law this means the impact of pore pressure on  $^R\sigma_1-\sigma_3$  is lower, hence  $\alpha < 1$ . The higher the confining pressure the stronger the effect – as proved by Gustkiewicz (1990) – for shale from the "Nowa Ruda" hard coal mine.

It should be emphasized that dilatant strengthening is not observable for absorptive liquid – here distilled water. Gustkiewicz et al. (2003) tested the same "Tumlin" sandstone and proved

that water – non-inert substance – decreases strength of the rock compared to dry rock. On the other hand the strength of rock strongly depends on capacity of absorbed fluid and in case of water it depends on pore pressure to a negligible extent. Hence the slight impact of pore water pressure on differential strength limit, manifested by close to unity  $\alpha$  coefficient.

Another key element of equation (15) is the so-called effective pressure value  $p'$ . During the aforementioned experiments the quantity has to be taken as the substitute confining pressure, which – in case of rock  $p_p = 0$  – returns the same  $^R\sigma_1 - \sigma_3$  value as the pair of non-zero pressures  $p$  and  $p_p$  satisfying the equation (15). Presented in fig. 7 relationships suggest that the  $p'$  quantity practically does not depend on the type of pore fluid. In other words: if  $p_p = 0$  then  $^R\sigma_1 - \sigma_3 = \text{const}$  for given  $p'$  regardless of what medium fills the pore space.

Such foregone conclusion, however, would have been an error. Research conducted at the Laboratory of Rock Deformation of IMG PAN into impact of pore fluid type on differential strength limit have proved on numerous occasions that even at zero pore pressure the pore fluid itself can lower that limit, often to a little degree though (see e.g. Gustkiewicz et al., 2003; Gustkiewicz, 1990). Pore fluid can reduce friction between failure surfaces thus increasing deformability of the rock. The aforementioned Rehbinder effect can also occur. It seems as if in the analysed case changes in  $^R\sigma_1 - \sigma_3$  caused by different pore fluids are small compared to irregularity of results caused by heterogeneity of tested material, hence the final form of relationships presented in fig. 7.

There are no doubts, however, over  $p'$  increasing simultaneously with increase in  $^R\sigma_1 - \sigma_3$ . Basically, the differential strength limit of the specimen is greater the greater is confining pressure applied to it. Thus, higher  $^R\sigma_1 - \sigma_3$  values are accompanied by higher  $p'$ .

Presented results were produced through research conducted within activities defined in the Charter of The Strata Mechanics Research Institute in Cracow financed by The Ministry of Science and Higher Education.

## References

- Biot M.A., 1941. *General theory of three dimensional consolidation*. J. Appl. Phys. 12: 155-168.
- Bluhm J., de Boer R., 1996. *Effective stress – clarification*. Arch. Appl. Mech., Vol. 66, pp. 479-492.
- de Boer R., Ehlers W., 1990. *The development of the concept of effective stresses*. Acta Mechanica, Vol. 83, pp. 77-92.
- de Boer R., 2005. *The Engineer and the scandal – a piece of science history*. Springer Verl., Berlin, 293 pages.
- Detournay E., Cheng, A.H.-D., 1993. *Fundamentals of Poroelasticity*. In: „Comprehensive Rock Engineering: Principles, Practice & Projects”, Vol. II, C. Fairhurst (ed.), Pergamon Press, 113-171.
- Dutka B., Lizak Z., Nowakowski A., Nurkowski J., Wierzbicki M., 2008. *Zależność wartości współczynnika Biota od rodzaju medium porowego*. W: Prace Instytutu Mechaniki Górotworu PAN, t. 10, z. 1-4, s. 3-16.
- Fabre D., Gustkiewicz J., 1998. *Influence of rock porosity on the Biot's coefficient*. In: “Poromechanics – A Tribute to Maurice A. Biot”, Proc. of the Biot Conf. on Poromech., Louvain-la-Neuve (Belgium), 14-16 Sept. 1998, Thimus et al. (eds.), Balkema, Rotterdam.
- Fillunger P., 1915. *Versuche über die Zugfestigkeit bei allseitigem Wasserdruck*. Österr. Wochenschrift für den öffentlichen Baudienst. Vol. 29, pp. 443-448.
- Fillunger P., 1914. *Neuere Grundlagen für die statische Berechnung von Talsperren*. Zeitschrift des Österr. Ing.- und Arch.- Vereines, Vol. 23, pp. 441-447.
- Fillunger P., 1913. *Der Auftrieb in Talsperren*. Österr. Wochenschrift für den öffentlichen Baudienst. Vol. 19, pp. 532-556; 567-570.

- Gustkiewicz J., 1990. *Deformacje i wytrzymałość skal w trójosiowym stanie naprężenia z uwzględnieniem płynów porowych*. W: „Górotwór jako ośrodek wielofazowy. Wyrzuty skalno-gazowe”, praca zbiorowa, J. Litwiniszyn (ed.), Wydawnictwo AGH, t. 1, s. 96-136.
- Gustkiewicz J., 1989. *Objętościowe deformacje skały i jej porów*. Arch. Min. Sci., Vol. 34, Issue 3, 593-609.
- Gustkiewicz J., Nowakowski A., 2004. *Deformacje i pękanie skal w warunkach laboratoryjnych*. Arch. Min. Sci., 49, Special Issue, 9-50.
- Gustkiewicz J., Nowakowski A., Nurkowski J., Stanisławski L., Lizak Z., 2004. *Kształtowanie się ciśnienia efektywnego w klasycznym, trójosiowym stanie naprężenia, na podstawie wyników pękania i deformacji wybranych skal*. Prace IMG PAN, t. VI, s. 3-17.
- Gustkiewicz J., Nowakowski A., Lizak Z., 2003. *Zmiany niektórych właściwości piaskowca pod wpływem sorbujących i niesorbujących płynów porowych pod ciśnieniem*. Prace IMG PAN, t. 5, nr 3-4, s. 367-375.
- Handin J., Hager R.V., Friedman M., Feather J.N., 1963. *Experimental deformation of sedimentary rocks under confining pressure: pore pressure tests*. Bull. Am. Assoc. Petr. Geol., Vol. 47, pp. 717-755.
- Hołda S., 1990. *Wpływ sorpcji gazów, par i cieczy na wytrzymałość skal*. W W: „Górotwór jako ośrodek wielofazowy. W: „Górotwór jako ośrodek wielofazowy. Wyrzuty skalno-gazowe”, praca zbiorowa, J. Litwiniszyn (ed.), Wydawnictwo AGH, t. 2, s. 443-453.
- Kovári K., Tisa A., Einstein H.H., Franklin J.A., 1983. *Suggested Methods for Determining the Strength of Rock Materials in Triaxial Compression: Revised Version*. Int. J. Rock Mech. Min. Sci. & Geomech. Abstr., Vol. 20, No. 6, pp. 283-290.
- Lade P.V., de Boer R., 1997. *The concept of effective stress for soil, concrete and rock*. Géotechnique, Vol. 47, No. 1, pp. 71-67.
- Nowakowski A., 2007. *On certain determinantal method of equation and effective pressure evaluation on the basis of laboratory researches*. Arch. Min. Sci., V. 52, No. 4, pp. 587-610.
- Nowakowski A., 2005. *Różne sposoby kształtowania się ciśnienia efektywnego w skale znajdującej się na granicy wytrzymałości*. Prace IMG PAN, t. 7, nr 3-4, s. 189-202.
- Nowakowski A., Młynarczuk M., Ratajczak T., Gustkiewicz J., 2003. *Wpływ warunków termicznych na zmianę niektórych właściwości fizycznych i strukturalnych wybranych skal*, Prace IMG PAN. Rozprawy, Monografie, nr 5, 104 s.
- Nur A., Byerlee J.D., 1971. *An Exact Effective Stress Law for Elastic Deformation of Rock with Fluids*. J. Geophys. Res., 76, 26, 6414-6419.
- Paterson M.S., Wong T.-f., 2005. *Experimental Rock Deformation – The Brittle Field*. Springer-Verlag Berlin Heidelberg, 347 pages.
- Rehbinder P., Lichtman V., 1957. *Effect of surface active media on strains and rupture in soils*. In: Electrical Phenomena and Soil/Liquid Interface. J. H. Schulman (ed.), Proc. 2<sup>nd</sup> Int. Congr. Surface Activity, Vol. III, London, Butterworths, 563-582.
- Rice J.R., Cleary M.P., 1976. *Some basic stress diffusion solutions for fluid-saturated elastic porous media with compressible constituents*. Reviews of Geophysics and Space Physics. 14(4): 227-241.
- Robin P.-Y.F., 1973. *Note on effective pressure*. J. Geophys. Res., 78, 2434-2437.
- Roegiers J.-C., Cui L., Bai M., 1978. *Poroelasticity applications*. In: Mechanics of Jointed and Faulted Rock. Proc. of the MJFR-3 Int. Conf., Vienna, 6-9 April 1998. Hans-Peter Rossmanith (ed.), Balkema, Rotterdam, 39-46.
- Terzaghi K., 1923. *Die Berechnung der Durchlässigkeitsziffer des Tones aus dem Verlauf der Spannungs-erscheinungen*. Sitzungsber. Akad. Wiss. Wien Math.-Naturwiss. Kl., Abt. 2A, 132, 105.
- Terzaghi K., 1936. *The shearing resistance of saturated soils and the angle between planes of shear*. In: Proc. Int. Conf. Soil Mech. And Found. Eng., Casagrande, A. & Rutledge P.C. & Watson J.D. (eds), Harvard University, Vol. I, pp. 54-56.
- Zienkiewicz O.C., Shiomi T., 1984. *Dynamic behaviour of saturated porous media; the generalized Biot formulation and its numerical solution*. Int. J. Num. Anal. Meth. Geomech. 8: 71-96.
- Zoback M.D., Byerlee J.D., 1975. *The effect of microcrack dilatancy on the permeability of Westerly granite*. J. Geophys. Res., 80, 752-755.